

**REVISED JPET/2013/207928**

**EFFECTS OF NITRIC OXIDE ON ANTICANCER ACTIVITY OF  
TOPOISOMERASE-ACTIVE DRUGS, ETOPOSIDE AND ADIAMYCIN, IN  
HUMAN MELONOMA CELLS**

Birandra K. Sinha, Ashutosh Kumar, Suchandra Bhattacharjee, Michael G. Espey, and Ronald  
P. Mason

Laboratory of Toxicology & Pharmacology, National Institutes of Environmental Health  
Sciences, Research Triangle Park, North Carolina 27709 and NIDDK, NIH, Bethesda,  
Maryland (MGE)

**Running Title Page:** Effects of NO on cytotoxicity of Etoposide and Adriamycin

Correspondence to Dr. Birandra K. Sinha at National Institutes of Environmental Health Sciences, Research Triangle Park, North Carolina 27709

Tel: (919)-541-4751

Fax: (919) 541-1043

*E-mail: [sinhal@niehs.nih.gov](mailto:sinhal@niehs.nih.gov)*

Text pages: 36

Figures: 6

Table: 2

Total references: 60

Word counts in Abstract: 214

Word counts in Introduction: 669

Word counts in Discussion: 1190

**Abbreviations:** iNOS, inducible nitric oxide synthase; •NO, nitric oxide; •NO<sub>2</sub>, nitrogen dioxide; VP-16; Etoposide; VP-16•, VP-16-pheoxyl radical; Adr, Adriamycin; top II, topoisomerase II; L-NIL, N<sup>6</sup>-(1-iminoethyl)-L-lysine hydrochloride; CYP, cytochrome P-450; HPLC, high performance liquid chromatography; DMSO, dimethylsulfoxide; MTT, microculture tetrazolium toxicity; PBS, phosphate buffered saline.

## ABSTRACT

Nitric oxide ( $\bullet$ NO) was originally identified as an innate cytotoxin. However, in tumors it can enhance resistance to chemotherapy and exacerbate cancer progression. Our previous studies have indicated that  $\bullet$ NO/ $\bullet$ NO-derived species react with etoposide (VP-16) in vitro and form products that show significantly reduced activity towards HL60 cells and lipopolysaccharide (LPS)-induced macrophages. Here, we further confirm the hypothesis that  $\bullet$ NO generation contributes to VP-16 resistance by examining interactions of  $\bullet$ NO with VP-16 in inducible nitric oxide synthase (iNOS)-expressing human melanoma A375 cells. Inhibition of iNOS catalysis by  $N^6$ -(1-iminoethyl)-L-lysine dihydrochloride (L-NIL) in human melanoma A375 cells reversed VP-16 resistance, leading to increased DNA damage and apoptosis.

Furthermore, we found that co-culturing A375 melanoma cells with LPS-induced macrophage RAW cells also significantly reduced VP-16 cytotoxicity and DNA damage in A375 cells. We also examined the interactions of  $\bullet$ NO with another topoisomerase active drug, Adriamycin, in A375 cells. In contrast, to VP-16,  $\bullet$ NO caused no significant modulation of cytotoxicity or adriamycin-dependent apoptosis, suggesting that  $\bullet$ NO does not interact with Adriamycin. Our studies support the hypothesis that  $\bullet$ NO oxidative chemistry can detoxify VP-16 through direct nitrogen oxide radical attack. Our results provide insights into the pharmacology and anticancer mechanisms of VP-16 that may ultimately contribute to increased resistance, treatment failure, and induction of secondary leukemia in VP-16-treated patients.

## INTRODUCTION

Topoisomerases constitute an important class of nuclear enzymes responsible for maintaining the topology and function of DNA. Inhibition and/or interference with topoisomerase functions lead to cell death. A large number of clinically active anticancer drugs (e.g., etoposide, adriamycin, and camptothecin) interact with and poison topoisomerases, causing significant DNA damage and cell death. Etoposide (VP-16), a topo II poison, is active against lung and testicular cancers and lymphoma (Henwood and Brogden, 1990). Adriamycin (Adr), also a topo II poison (Liu, 1988), is active against a wide range of cancers, including leukemias, bladder, breast, lung and multiple myelomas (Sinha, 1995).

VP-16 is rapidly metabolized by CYPs and peroxidases to *o*-dihydroxy- and *o*-quinone derivatives of VP-16 (Haim et al., 1986, 1987a,b; VanMaanen et al., 1987; Kalyanaraman et al., 1989; Kagan et al., 2001), and the formation of these metabolites requires the generation of a VP-16 radical (VP-16<sup>•</sup>) formed from the oxidation of the 4'-OH group of VP-16 (Haim et al., 1987a,b). VP-16 metabolites bind to cellular components (Haim et al., 1986, 1987a) and cause DNA strand cleavage through a topo II-mediated mechanism (Sinha et al., 1990; Gantchev and Hunting, 1998). VP-16<sup>•</sup> causes oxidative stress both *in vitro* and *in vivo* by oxidizing glutathione and forming the glutathione thiol radical (Katki et al., 1987). In addition, VP-16-*o*-quinone has been reported to form glutathione adducts in HL60 cells (Fan et al., 2006).

Adriamycin has been reported to intercalate into DNA and binds covalently to DNA and proteins via generation of reactive species through reductive bioactivation (Sinha, 1980; Sinha et al., 1984). Reductive activation also generates free radicals via the formation of

semiquinone radical and its reaction with molecular oxygen (Kalyanaraman et al., 1980; Myers et al., 1987; Sinha et al., 1987). While the covalent binding to DNA and formation of free radicals are implicated in the mechanisms of Adr cytotoxicity (Myers et al. 1987, Sinha et al. 1987) and cardiotoxicity (Dorowshow 1983; Rajagopalan et al., 1988), poisoning of topo II is considered to play a significant role in tumor cell death.

$\bullet$ NO and/or its products ( $\bullet$ NO<sub>2</sub>, ONOOH) have been shown to play significant roles in cancer biology, including the innate immune response, neovascularization, cancer metastasis and cell death (Jenkins et al., 1995; Wink et al., 1998a; Xu et al., 2002; Chen et al., 2008). Exposure to  $\bullet$ NO (via NO donors) modifies activities of certain anticancer drugs including Adr (Cook et al., 1997; Evig et al., 2004; Wink et al., 1997b).  $\bullet$ NO and/or its products react with a wide variety of substrates including amines, thiols and phenols (Janzen et al., 1993; Cudic and Ducrocq, 2000; Yenes and Messegueur 1999).  $\bullet$ NO-derived species rapidly react with phenols to form phenoxy radicals, quinones and nitrated phenols. The formation of nitrotyrosine in cellular proteins has been associated with modifications of protein activities (Curtis et al., 1996; Chatterjee et al., 2009). Furthermore,  $\bullet$ NO has been reported to react with the tyrosyl radical of ribonucleotide reductase, resulting in the inhibition of DNA synthesis and, ultimately, cell death (Lepovre et al., 1994)

VP-16 contains a phenolic OH group in the 4'-position, and both the cytotoxicity and the binding of VP-16 to topo II are dependent upon the presence of this moiety (Loike and Horwitz, 1976; Long et al., 1984; Sinha et al., 1990). We have recently shown that the phenolic OH of VP-16 reacts with  $\bullet$ NO-derived species to generate VP-16 $\bullet$ , *o*-quinone, and

other products, thereby modulating the cytotoxicity of VP-16 towards cancer cells (Sinha et al., 2013). In this report, we have further examined the interactions of VP-16 and Adr with endogenously formed  $\bullet$ NO via iNOS catalysis in A375 human melanoma cells. Our results support the conclusion that the reaction of  $\bullet$ NO with VP-16 diminishes its cytotoxic activity towards cancer cells. In contrast, endogenously formed  $\bullet$ NO in A375 cells had no significant effects on Adr cytotoxicity, indicating that Adr did not interact with  $\bullet$ NO or  $\bullet$ NO-derived species. This work extends our *in vitro* work to the cellular systems and confirms the same processes observed for VP-16 *in vitro* also operates in tumor cells.

**Materials and Methods:** VP-16 and Adriamycin were the gift of the Drug Synthesis and Chemistry Branch, Development Therapeutic Program of NCI, NIH. Human topoisomerases and SDS/KCl precipitation assay kits were obtained from Topogen (Columbus, Ohio). The nitric oxide synthase (inducible, iNOS) inhibitor,  $N^6$ -(1-iminoethyl)-L-lysine dihydrochloride (L-NIL) was obtained from Cayman Chemicals. Caspase-3 activity was measured by an Abcam assay kit (Cambridge, MA). A primary antibody for the analysis of iNOS was obtained from Santa Cruz Biotech, CA. A nitric oxide assay kit was purchased from Thermo Scientific (Waltham, MA).

**Cytotoxicity Studies:** A375 melanoma cell lines and macrophage RAW 264.7 cells (ATCC, Rockville, Maryland) were grown in Phenol-red free RPMI media supplemented with 10% fetal bovine serum and antibiotics. A375 cells and RAW 264.7 were used for 15 passages, after which the cells were discarded and a new cell culture was started from fresh frozen stock.

The intracellular reaction between VP-16 and endogenous  $\bullet$ NO was examined in A375 cells by pre-incubating cells either in the presence or absence of an iNOS inhibitor (L-NIL) for 4 h prior to the addition of VP-16. A375 cells (2000/well) were plated in Phenol Red-free medium and cultured for 96 hrs. DMSO was included as the vehicle control and the cytotoxicity was measured by the MTT assay as described (Alley et al., 1988).

Co-culture experiments for cytotoxicity with A375 cells and induced RAW cells were carried out in 6-well plates separated by 0.4  $\mu$ M membrane filters (Costar, Corning, NY).

Macrophage RAW cells were induced as described previously (Sinha et al., 2013). For the cytotoxicity studies, 200,000-250,000/well of A375 cells were plated in 3 ml of complete medium into a 6-well plate (in duplicates) and allowed to attach for 4-6 hrs. Membranes were inserted and various concentrations of VP-16 were added onto the top of membranes containing LPS-induced cells ( $1 \times 10^6$ ) and incubated for 48 hrs. Membranes and RAW cells were removed, A375 cells were washed once with ice-cold PBS, trypsinized, and the cytotoxicity was determined by counting the cells. Nitrite concentrations were determined using Greiss reagent as described previously (Sinha et al., 2013).

**Western Blot Assay:** Samples (10  $\mu$ g of total protein) were electrophoresed under reducing conditions through 4-12% Bis-Tris NuPage acrylamide gels (Invitrogen, Carlsbad, CA). After electrophoresis, proteins were transferred onto a nitrocellulose membrane and probed with anti-iNOS and anti-beta actin antibodies. An Odyssey infrared imaging system (Li-Cor

Biosciences, Lincoln, NE) was used to acquire images. Rabbit polyclonal anti-iNOS antibody was used to quantitate iNOS proteins in samples using a standard ELISA (Ranguelova et al., 2008).

**Caspase-3 Assay:** Caspase-3 activity in A375 cell lysate was measured by a colorimetric assay kit (Abcam, Cambridge, MA) using the manufacturer's instructions. Briefly, one million cells were treated with VP-16 (25  $\mu$ M and 50  $\mu$ M) in the presence or absence of L-NIL (250-400  $\mu$ M) for 18 h. Cells were collected by centrifugation and lysed with the lysis buffer (Abcam) by incubating for 10 minutes on ice. Cells were centrifuged at 10,000 x g for 5 minutes, supernatant was collected, and the protein concentration was determined by the BCA assay. Equal amounts of the protein (200-400  $\mu$ g) were incubated with 10 mM DTT containing the reaction buffer, followed by the addition of Caspase-3 substrate (DEVD-Pna, 4 mM), and the reaction mixture was incubated at 37°C for 2-4 h. The sample was analyzed for absorbance at 405 nm in a multiwell plate reader and results expressed as substrate utilization per mg protein.

**SDS-KCl Precipitation Assay:** The formation of covalent topo II/DNA complexes with VP-16 in the presence or absence of L-NIL was quantitated by the SDS-KCl precipitation assay as described before (Liu et al., 1983). Briefly, DNA of A375 cells growing in the logarithmic phase ( $2 \times 10^6$  /ml) was labeled with [methyl- $^3$ H]-thymidine (10 $\mu$ ci, 2Ci/mmol; Perkin-Elmer) for 18-24 h. Cells were collected and washed twice with the medium, diluted in fresh medium and seeded into a six-well plate at a density of  $2 \times 10^5$  cells/ml. L-NIL was pre-incubated with

the cells for 18 h during the labeling phase. VP-16, dissolved in DMSO, was added and incubated for 1 h. Cells were washed with PBS (2 x) and lysed with 1 ml of pre-warmed lysis solution (Topogen). After lysis and shearing of DNA, DNA-Topo II-VP-16 complexes were precipitated with KCl. The precipitate was collected by centrifugation and washed extensively (four times) with the washing solution (Topogen) according to the manufacturer's instructions. The radioactivity was counted in a scintillation counter after adding 5 ml of scintillation fluid.

The effects of endogenously generated •NO from iNOS of LPS-induced macrophage RAW cells on SDS-KCl precipitate formation in A375 cells were investigated as described in the cytotoxicity studies, except that the drug exposure was for 90 minutes, and samples were processed for the SDS-KCl precipitation assay as described above. In some experiments, VP-16 (10  $\mu$ M) was pre-incubated with LPS-induced RAW cells ( $0.5 \times 10^6$  cells/ml, 30 minutes), the mixtures added to 6-well plates fitted with membrane filters (on top) and allowed to interact with the  $^3$ H-labeled A375 cells (in bottom, 200-250,000 cells/well) for 90 minutes. Medium was removed and the cells washed once with PBS, A375 cells were lysed with pre-warmed lysis buffer, and the samples were processed as described above.

**Metabolism of VP-16 in A375 Cells:** The metabolic studies with VP-16 in A375 cells in the presence and absence of L-NIL were carried out similarly to those described previously (Haim et al., 1987a, b). Briefly,  $1 \times 10^6$ /ml cells in 5 ml of Phenol red-free media were seeded in a 100 x 15 mm petri dish (Falcon, Becton, Dickinson and Company, Franklin Lakes, NJ) and

were allowed to attach for 4 h. L-NIL (400  $\mu$ M) was added to the cells and incubated for 18 h before VP-16 (100  $\mu$ M) was added at various time points. At the end of the incubation, cells were washed with ice-cold PBS (5 ml), gently scraped in 5 ml of ice-cold PBS, and collected by centrifugation (2000g, 5 min). The cells were suspended in 1 ml of ice-cold PBS, lysed with sonication (4°C) and the resulting mixture extracted with chloroform (4 x 1 ml). The combined organic layers were removed under argon, and the residue was dissolved in 200  $\mu$ l of methanol and analyzed by HPLC as described previously (Haim et al., 1987a, b), except that a C18 column was used and MeOH-Water (60:40) was the mobile phase. Under these conditions, VP-16 and VP-16-*o*-quinone had retention times of 2.1 min and 2.7 min, respectively.

## RESULTS

Using purified topo II enzyme, we had previously reported that products formed from reactions of  $\bullet$ NO and/or  $\bullet$ NO-derived species with VP-16 were significantly less active than the parent drug in inducing DNA cleavage and were not cytotoxic to HL60 cells (Sinha et al., 2013). In this report we examined whether endogenous formation of  $\bullet$ NO catalyzed by iNOS in cancer cells could affect the cytotoxicity of VP-16 and Adr. To assess this, we used a human melanoma A375 tumor cell line which has been shown to express iNOS and to produce levels of  $\bullet$ NO that are relatively low (Tang and Grimm, 2004; Chanvorachote et al., 2006; Sikora et al., 2010). The presence of iNOS was confirmed in A375 cells with a primary antibody for iNOS (Figure 1A), and our results are similar to those described previously (Sikora et al., 2010). Furthermore, treatment of A375 cells with 10 ng/ml LPS for 18 h

significantly induced this protein, further confirming the presence of the inducible form of NOS in A375 cells (Figure 1B). It is interesting to note that under these experimental conditions, formation of  $\bullet\text{NO}/\text{NO}_2$  was not detected by the Griess reaction (data not shown). This observation is similar to those previously published by Sikora et al., (2010) and Chin and Deen (2010), as the amount of NO synthesis in A375 cells is well below (100-150 nM) the detection limits of the Griess reaction.

Examination of caspase-3 activity, a marker for apoptosis, in A375 cells showed that VP-16 alone (25  $\mu\text{M}$  and 50  $\mu\text{M}$ ) induced 2.5-fold and 3.5-fold increases in caspase-3 activity, respectively, after 18 h (Figure 2, Panel A). Inhibition of iNOS with L-NIL (400  $\mu\text{M}$ ) further enhanced caspase-3 activity 4.5-fold and 6.0-fold in the presence of 25  $\mu\text{M}$  and 50  $\mu\text{M}$  VP-16, respectively. Consistent with these data, application of L-NIL (400  $\mu\text{M}$ ) significantly enhanced VP-16 cytotoxicity in A375 cells (2.5-3.5-fold; Figure 2, Panel B). The relative  $\text{IC}_{50}$  (concentration required to inhibit cell growth by 50%) is presented in Table 1. Under these conditions, L-NIL alone had no significant effect on caspase-3 activity or A375 cell viability.

Since LPS significantly induced iNOS (Figure 1), we examined the cytotoxicity of VP-16 following induction of A375 cells with LPS. Consistent with the increase in the expression of iNOS, VP-16 cytotoxicity was further decreased in the induced A375 cells (Figure 3A and Table 1). More interestingly, the presence of L-NIL significantly sensitized A375 cells to VP-16 (Figure 3A and Table 1), suggesting that increased  $\bullet\text{NO}$  formation from iNOS was responsible for the decrease in VP-16 cytotoxicity in A375 cells. To further examine the roles

of exogenously generated  $\bullet\text{NO}$  on VP-16 cytotoxicity in A375 cells, we carried out co-culture studies with LPS-induced macrophage RAW cells. As shown (Figure 3B and Table 1), exogenously formed  $\bullet\text{NO}$  from iNOS in RAW cells further decreased VP-16 cytotoxicity (> 15-fold), suggesting that  $\bullet\text{NO}$  generated from the induced RAW cells reacted with VP-16 and formed non-cytotoxic species. Additionally, data presented in Table 2 show that considerable amounts of  $\bullet\text{NO}$  were generated from the induced RAW cells and the presence of VP-16 (in co-culture cytotoxicity studies) significantly decreased  $\bullet\text{NO}$  formation, indicating reaction between VP-16 and  $\bullet\text{NO}$ . Furthermore, there were no significant differences in nitrite formation between the top and bottom layers (compartments) of the six-well plates, suggesting free diffusion of  $\bullet\text{NO}$  across the membrane. In contrast, the cytotoxicity of VP-16 was not significantly affected (data not shown) in the presence of non-induced RAW cells, indicating that  $\bullet\text{NO}/\bullet\text{NO}$ -species generated in the induced RAW cells from iNOS catalysis were responsible for this decrease in VP-16 cytotoxicity.

Adriamycin is a topo II-active drug that induces protein-associated DNA damage leading to cell death and, thus, is similar to VP-16 in its mode of action. We therefore, examined the effects of endogenously generated  $\bullet\text{NO}$  in Adr-induced apoptosis and cytotoxicity in A375 cells. Under similar conditions, the presence of L-NIL had no significant effects on caspase-3 activity induced by Adr (Figure 4). Furthermore, the presence of L-NIL had no effects on the cytotoxicity of this drug (Figure 4) in A375 cells. These observations would indicate that Adr does not react with  $\bullet\text{NO}/\bullet\text{NO}$ -related species.

**Effects of L-NIL on VP-16-Induced Cleavable Complex in A375 Cells:** To determine whether iNOS catalysis influences the formation of a VP-16/topo II complex, we evaluated the formation of the cleavage complex by VP-16 in the presence of L-NIL using an SDS/KCl precipitation assay (Liu et al. 1983). As expected, treatment of A375 cells with VP-16 (10  $\mu$ M) significantly increased (6-7-fold) the formation of the SDS/KCl precipitate (Figure 5) over the untreated controls. The presence of L-NIL further increased this complex formation (10-fold), equivalent to the effects of VP-16 alone at 5 times the concentration (50  $\mu$ M; Figure 5). This result suggests that inhibition of  $\bullet$ NO formation in A375 cells by L-NIL increased the DNA damage induced by VP-16 in a topo II-dependent manner.

In order to further confirm that  $\bullet$ NO or  $\bullet$ NO-derived species were responsible for this decrease in VP-16-mediated topo II-dependent DNA damage, we carried out co-culture experiments with induced macrophage RAW cells. Co-incubation of A375 cells with induced RAW cells significantly decreased VP-16-dependent SDS-KCl precipitate formation (Figure 5B). Similar effects were noted when the co-incubations were carried out either simultaneously or with pre-incubated VP-16 (Figure-5B). Taken together, these observations strongly suggest that  $\bullet$ NO and associated nitrogen oxides can react with VP-16, thereby making it less effective at inducing apoptosis and DNA damage, and resulting in increased VP-16 resistance towards cancer cells.

**Metabolism of VP-16 in A375 Melanoma Cells:** In order to examine the effects of endogenously produced  $\bullet$ NO on VP-16 metabolism in A375 cells, VP-16 was incubated with

A375 cells for various times in the presence or absence of L-NIL. HPLC analysis (Figure 6) clearly indicated that VP-16 is rapidly metabolized in A375 cells, and a significant amount of VP-16-*o*-quinone was formed within 15 minutes of incubation. The presence of L-NIL completely inhibited the quinone formation, indicating that  $\bullet$ NO and other nitric oxide species formed from iNOS in A375 cells were responsible for the *o*-quinone formation.

## DISCUSSION

The impact of NOS activity on tumor biology is diverse and dependent on a myriad of host factors (Ambs and Glynn, 2011). Likewise,  $\bullet$ NO and its nitrogen oxide products can affect cancer therapy either positively or negatively (Hickok and Thomas, 2010). The present study extends our work in vitro to tumor cells and shows significant oxidative chemistry of  $\bullet$ NO with VP-16.

In our previous study we showed that the reaction of  $\bullet$ NO/NO species with VP-16 initiates through the obligate intermediacy of the 4'-phenoxy radical, with subsequent formation of *o*-quinone and short-lived VP-16 nitrogen oxide species (Sinha et al., 2013).  $\bullet$ NO reacts with phenolic compounds (Janzen et al., 1993, Cudic and Ducrocq, 2000, Yenes and Messeguer, 1999), and the initiator in these reactions is believed to be the autoxidation of  $\bullet$ NO (Liu et al., 1998; Espey et al., 2001) with the formation of the  $\bullet$ NO<sub>2</sub> radical, which can attack the electron-rich phenolic OH group to generate the phenoxyl radical (Hogg et al., Goss et al., 1999).

Interaction of VP-16 with topo-II has been shown to cause both single- and double-strand DNA breaks (Long et al., 1984, Glisson et al., 1986; Sinha et al., 1988), which, in the absence of DNA repair, results in cell death. Indeed, a significant decrease in VP-16-dependent DNA damage and cell death has been observed in cell lines where the activity of topo-II had been compromised (Glisson et al., 1986; Sinha et al., 1988). Our previous studies have clearly shown that products of VP-16 exposed to  $\bullet\text{NO}$  (in the presence of  $\text{O}_2$ ) were no longer cytotoxic to HL60 cells and lacked sufficient ability to induce topo II-dependent DNA damage (Sinha et al., 2013).

To further address the relevance of this  $\bullet\text{NO}$  chemistry observed *in vitro*, iNOS-expressing human melanoma A375 cells were utilized to directly elucidate the role of  $\bullet\text{NO}$  in the cytotoxicity of VP-16. Our present studies clearly show that inhibition of formation of  $\bullet\text{NO}$  (and  $\bullet\text{NO}$ -related species) by L-NIL increased caspase-3-dependent apoptosis by VP-16 (2-fold), with a concomitant increase (2.5-3.5-fold) in VP-16 cytotoxicity to A375 tumor cells (Figure 2A & B and Table 1). Induction of iNOS in A375 cells with LPS further decreased VP-16 cytotoxicity in A375 cells. Interestingly, inhibition of  $\bullet\text{NO}/\bullet\text{NO}$ -related species by L-NIL resulted in sensitization of cells to VP-16. These studies taken together strongly suggest that  $\bullet\text{NO}/\bullet\text{NO}$ -related species react with VP-16 and generate products that are significantly less cytotoxic to A375 cells.

Co-culture studies carried out with LPS-activated macrophage RAW cells (which generate large quantities of  $\bullet\text{NO}/\bullet\text{NO}$ -related species) show a further (> 15-fold) decrease in VP-16 cytotoxicity to A375 cells. This is a very significant finding, as this decrease in VP-16

cytotoxicity in the presence of exogenously generated  $\bullet$ NO from macrophage cells is quite large compared to that found with endogenously generated  $\bullet$ NO from iNOS catalysis in A375 cells (2.5-3.5-fold). Our findings would suggest that even in those cancer cells expressing low levels of iNOS, infiltrating macrophages would further increase VP-16 resistance by increasing detoxification of VP-16 via  $\bullet$ NO-dependent chemistry. In tumors, the presence of macrophages is well established, and they play significant roles in tumor progression, neovascularization and poor survival (Jenkins et al., 1995; Ambs and Glynn, 2011; Lewis and Pollard, 2006; Pollard, 2008).

Nitric oxide has been reported to stabilize Bcl2, resulting in decreased cytotoxicity of *cis*-platinum in A375 cells (Tang and Grimm, 2004; Chanvorachote et al., 2006), thus raising the possibility of a general apoptotic resistance mechanism for  $\bullet$ NO independent of direct VP-16 reactions. However, the current study shows that endogenously/exogenously formed  $\bullet$ NO (or  $\bullet$ NO-derived species) reacts with VP-16 to generate less active metabolites of VP-16, resulting in a decrease in both topo II-mediated DNA damage and cytotoxicity. In contrast, L-NIL had no significant effects on Adriamycin-induced apoptosis or cytotoxicity in A375 cells, which would indicate that Bcl2 did not play a role in VP-16 activity.

Inhibition of cellular  $\bullet$ NO formation by L-NIL caused an increase in intracellular unmodified VP-16, resulting in increased DNA damage and cytotoxicity. Our observations with Adr further confirm that L-NIL did not affect apoptosis nor did it significantly affect its cytotoxicity. Similar observations were also noted with Camptothecin, a topo I-active drug, where the presence of L-NIL had no significant effect on caspase-3 activity or its cytotoxicity

in A375 cells (unpublished observations), lending support to the conclusion that L-NIL did not modulate VP-16 pharmacology by non-specific effects on caspase-3 or topo II activities. We conclude, therefore, that iNOS catalysis within A375 tumor cells was sufficient to directly detoxify active VP-16 via  $\bullet\text{NO}/\bullet\text{NO}_2$ -dependent oxidative reactions.

$\bullet\text{NO}$  readily partitions into a hydrophobic medium, such as the interior of membranes (Liu et al., 1998). This, in combination with a relatively high rate of  $\bullet\text{NO}$  generation from iNOS catalysis, facilitates  $\bullet\text{NO}$  autooxidation and formation of  $\bullet\text{NO}_2$  (Hogg et al., 1996; Goss et al., Moller et al., 2007). The organic solubility of VP-16 may likewise localize and enhance interactions with reactive nitrogen oxides. The occurrence of both augmented iNOS catalysis (Ambs and Grimm, 2011) and alterations in cancer cell plasma membrane architecture (Moller et al, 2007; Zhuang et al., 2002; Miersch et al., 2008) will significantly influence iNOS-dependent detoxification of VP-16 and resistance towards cancer cells.

While in human patients VP-16 is exclusively metabolized by Cyp3A4 in the liver to its dihydroxy derivative, it is possible that VP-16 could also be metabolized by Cyp3A4 in A375 melanoma cells to the catechol derivative and *o*-quinone. While the roles of Cyp3A4 in A375 cells were not investigated in the present study, inhibition of *o*-quinone formation by L-NIL would suggest that  $\bullet\text{NO}$  was involved in its formation in A375 cells. The formation of the *o*-quinone was rapid and decreased significantly with time, suggesting binding to proteins and DNA. The formation of VP-16-*o*-quinone by  $\bullet\text{NO}$ -dependent pathways is very significant in light of the role of the quinone in the induction of acute myeloid leukemia in patients treated with VP-16. It has been reported that VP-16 metabolites increase topo II-dependent cleavage

near leukemia associated MLL translocation breakpoints (Lovett et al., 2001). Furthermore, Vlasova et al. (2011) have shown that VP-16 radical formed from one-electron oxidation can redox-cycle, leading to enhanced topo II-mediated strand breaks and MLL gene translocation. Our previous studies have shown that VP-16 is readily oxidized by  $\bullet\text{NO}$  chemistry to its phenoxy radical, an obligatory intermediate in the formation of the VP-16-*o*-quinone (Sinha et al., 2013).

We conclude, therefore, from our findings that  $\bullet\text{NO}$  oxidative chemistry occurs in A375 cancer cells and can detoxify VP-16. Our results provide insights into the pharmacology and anticancer activities of VP-16 in tumors that may ultimately contribute to increased resistance and treatment failure. VP-16 is currently used for the treatment of a variety of cancers (e.g., lung, melanoma, and breast) which are known to express iNOS (Grimm et al., 2008; Chen et al., 2008). It is tempting to suggest that the use of VP-16 and related anticancer drugs capable of reacting with  $\bullet\text{NO}/\bullet\text{NO}_2$  may be ill-advised for patients harboring cancers with intensive iNOS- activity. Furthermore, in tumors that do not express significant amounts of iNOS, infiltrating macrophages may further detoxify VP-16 and render tumor cells resistant to VP-16 as shown in our studies with melanoma cells.

**Acknowledgment:** The authors thank Ms. Mary J. Mason and Dr. Ann G. Motten for their careful review of the manuscript. The authors also thank Drs. Michael Waalkes and Fiona Summers for their critical review of the manuscript.

**Authorship Contributions:**

Participated in research design: Sinha, Kumar, Bhattacharjee, and Mason

Conducted experiments: Sinha, Kumar and Bhattacharjee

Contributed to new reagents or analytical tools: Kumar and Bhattacharjee

Performed data analysis: Sinha, Kumar, Bhattacharjee and Espey

Wrote or contributed to writing of the manuscript: Sinha and Mason

## REFERENCES

- Alley MC, Scudiero DA, Monks A, Hursey ML, Czerwinski MJ, Fine, DL, Abbott BJ, Mayo JG, Shoemaker RH, and Boyd MR (1988) Feasibility of drug screening with panels of human tumor cell lines using a microculture tetrazolium assay. *Cancer Res* 48: 589-601.
- Ambs S, and Glynn SA (2011) Candidate pathways linking inducible nitric oxide synthase to a basal-like transcription pattern and tumor progression in human breast cancer. *Cell Cycle* 10:619-624.
- Chatterjee S, Lardinois O, Bonini MG, Bhattacharjee S, Stadler K, Corbett J, Deterding LJ, Tomer KB, Kadiska M, and Mason RP (2009) Site-specific carboxypeptidase B1 tyrosine nitration and pathophysiological implications following its physical association with nitric oxide synthase-3 in experimental sepsis. *J Immunology* 183:4055-4066.
- Chanvorachote P, Ninmannit U, Stehlik C, Wang L, (2006) Nitric oxide regulates cell sensitivity to cisplatin-induced apoptosis through S-nitrosylation and inhibition of Bcl2 ubiquitination. *Cancer Res.* 66:6353-6350.
- Chen GG, Lee TW, Xu H, Yip JHY, Li M, Mok TSK, and Yim ARC (2008) Increased inducible nitric oxide synthase in lung carcinoma of smokers. *Cancer* 112: 372-381.
- Chin MP, and Deen WM (2010) Prediction of nitric oxide concentrations in melanoma *Nitric oxide-Biology and Chemistry* 23:319-326.
- Cook JA, Krishna MC, Pacelli R, DeGraff W, Liebmman J, Mitchell JB, Russo A, and Wink DA (1997) Nitric oxide enhancement of melphalan-induced cytotoxicity. *Br J Cancer* 76:325-334.

- Cudic M, and Ducrocq C (2000) Transformations of 2,6-diisopropylphenol by NO-derived nitrogen oxides, particularly peroxynitrite. *Nitric oxide-Biology and Chemistry* 4:147-156.
- Curtis JF, Reddy NG, Mason RP, Kalyanaraman B, and Eling TE (1996) Nitric oxide: A prostaglandin H synthase 1 and 2 reducing co-substrate that does not stimulate cyclooxygenase activity or prostaglandin expression in Murine macrophages. *Arch Biochem Biophys* 335: 369-376.
- Dorowshow JH (1983) Effects of anthracyclines antibiotics-stimulated superoxide, hydrogen peroxide and hydroxyl radical production by NADH dehydrogenase. *Cancer Res.*, 43: 4543-4551.
- Espey MG, Miranda KM, Thomas DD, and Wink DA (2001) Distinction between nitrosilating mechanisms within human cells and aqueous solutions. *J. Biol. Chem.* 276: 30085-30091.
- Evig CB, Kelley EE, Weydert CJ, Chu Y, Buettner GR, and Burns CP (2004) Endogenous production and exogenous exposure to nitric oxide augment doxorubicin cytotoxicity for breast cancer cells but not cardiac myoblasts. *Nitric Oxide-Biology and Chemistry* 10: 119-129.
- Fan Y, Schreiber EM, Giorgianni A, Yalowich JC, and Day BW (2006) Myeloperoxidase-catalyzed metabolism of etoposide to its quinone and glutathione adduct forms in HL60 cells. *Chem Res Toxicol* 19: 937-943.
- Gantchev TG, and Hunting DJ (1998) The ortho-quinone metabolite of the anticancer drug etoposide (VP-16) is a potent inhibitor of the topoisomerase II-DNA cleavable complex. *Mol Pharmacology* 53:422-428.

- Glisson B, Gupta R, Smallwood-Kentro S, and Ross WE (1986) Characterization of acquired epipodophyllotoxin resistance in Chinese-Hamster Ovary cell-line: loss of drug-stimulated DNA cleavage activity. *Cancer Res* 46:1934-1938.
- Goss SPA, Singh RJ, Hogg N, and Kalyanaraman, B (1999) Reactions of  $\bullet\text{NO}$ ,  $\bullet\text{NO}_2$  and peroxyntirite in membranes: Physiological implications. *Free Rad Res* 31:597-606.
- Grimm EA, Ellerhorst J, Tang CH, and Ekmekcioglu S (2008) Constitutive intracellular production of iNOS and NO in human melanoma: possible role in regulation of growth and resistance to apoptosis. *Nitric oxide-Biology and Chemistry* 19: 133-137.
- Haim N, Nemec J, Roman J, and Sinha BK (1986) Peroxidative free radical formation and *o*-demethylation of etoposide (VP-16) and teniposide (VM-26). *Biophys Biochem Res Commun* 135: 215-220.
- Haim N, Nemec J, Roman J, and Sinha BK (1987) Peroxidase-catalyzed metabolism of etoposide (VP-16-213) and covalent binding of reactive intermediates to cellular macromolecules. *Cancer Res* 47:5835-5840.
- Haim N, Nemec J, Roman J, and Sinha BK (1987) In vitro metabolism of etoposide (VP-16-213) by liver microsomes and irreversible binding of reactive intermediates to microsomal proteins. *Biochem Pharmacology* 36:527-536.
- Henwood JM, and Brogden JM (1990) Etoposide. A review of its pharmacodynamics and pharmacokinetic properties, and therapeutic potentials in combination therapy of cancer. *Drugs* 39: 438-490.
- Hickok JR, and Thomas DD (2010) Nitric oxide and cancer therapy: the emperor has NO clothes. *Curr Pharm Res* 16:381-391.

- Hogg N, Singh RJ, Goss SPA, and Kalyanaraman B (1996) The reaction between nitric oxide and a-tocopherol: a reappraisal. *Biochem Biophys Res Commun* 224: 696-702.
- Jenkins DC, Charles IG, Thomsen LL, Moss DW, Holmes LS, Baylis SA, Rhodes P, Westmore K, Emson PC, and Moncada S (1995) Roles of nitric oxide in tumor growth. *Proc. Natl. Acad. Sci. USA* 92: 4392-4396.
- Janzen EG, Wilcox AL, and Manoharan V (1993) Reactions of nitric oxides with phenolic antioxidants and phenoxy radicals. *J. Org. Chem.* 58:3597-3599.
- Kagan VE, Kuzmenko AI, Tyurina YY, Shvedova AA, Matsura T, and Yalowich JC (2001) Pro-oxidant and antioxidant mechanisms of etoposide in HL-60 cells: Role of myeloperoxidase. *Cancer Res* 61: 7777-7784.
- Kalyanaraman, B, Perez-Reyes, E, and Mason, RP (1980) Spin-trapping and direct electron resonance investigation of the redox metabolism of quinone anticancer drugs. *Biochem. Biophys. Acta* 630: 119-130.
- Kalyanaraman B, Nemec J, and Sinha BK (1989) Characterization of free radicals produced during oxidation of etoposide (VP-16) and its catechol and quinone derivatives: an ESR study. *Biochemistry* 28:4830-4846.
- Katki AG, Kalyanaraman B, and Sinha BK (1987) Interactions of the antitumor drug, etoposide with reduced thiols in vitro and in vivo. *Chem-Biol Interact* 62:237-247.
- Lewis CE, and Pollard JW (2006) Distinct role of macrophages in different tumor microenvironments. *Cancer Res* 66: 605-612.
- Lepoivre M, Flaman JM, Bobe P, Lemaire G, and Henery, Y (1994) Quenching of the tyrosyl free-radical of ribonucleotide reductase by nitric oxide-relationship to cytostasis induced in tumor-cells by cytotoxic macrophages. *J Biol Chem* 269: 21891-21897.

- Liu LF (1988) DNA topoisomerases poisons as antitumor drugs. *Ann Rev Biochem* 58: 351-375.
- Liu LF, Rowe TC, Yang L, Tewey KM and Chen GL (1983) Cleavage of DNA by mammalian topoisomerase-II. *J Biol Chem* 258: 5365-5370.
- Liu X, Miller MJ, Joshi MS , Tomas DD, and Lancaster JR (1998) Accelerated reactions of nitric oxide with O<sub>2</sub> within hydrophobic interior of biological membranes. *Proc Natl Acad Sci USA* 95:2175-2179.
- Loike JD, and Horwitz SB (1976) Effects of VP-16-213 on the intracellular degradation of DNA in HeLa cells. *Biochemistry* 15:5448-5453.
- Long BH, Musial ST, and Brattain MG (1984) Comparison of cytotoxicity and DNA breakage of congeners of phodophyllotoxin including VP-16-213 and VM-26: a quantitative structure-activity relationship. *Biochemistry* 23:1183-1188.
- Lovett BD, Strumberg D, Blair IA, Pang SK, Burden DA, Megonigal MD, Rappaport EF, Rebbeck TR, Osheroff N, Pommier YG, and Felix CA (2001) Etoposide metabolite enhances DNA topoisomerase II cleavage near leukemia-associated MLL translocation breakpoints. *Biochemistry*, 40: 1159-1170.
- Miersch S, Espey MG, Chaube, R, Akarca A, Tweten R, Anavaranich S, and Mutus B (2008) Plasma membrane cholesterol content affects nitric oxide diffusion dynamics and signaling. *J Biol Chem* 283:18513-18521.
- Moller MN, Li Q, Vittur DA, Robinson JM, Lancaster JR, and Denicola A (2007) Membrane lens effect: focusing the formation of reactive nitrogen oxides from •NO/O<sub>2</sub> reactions. *Chem Res Toxicol* 20:709-714.

- Myers CE, Mimnuagh E, Yeh G, and Sinha BK (1987) Biochemical Mechanism of Tumor Cell Kill by the Anthracyclines in Anthracyclines and Anthracenedione-based Anticancer Agents. (W.Lown, Ed.) pp527-569 , Elsevier Publisher, NY.
- Pollard JW (2008) Macrophages define the invasive microenvironment in breast cancer. *J. Leukocyte Biol* 84: 623-630.
- Rajagopalan S, Politi PM, Sinha BK, and Myers CE. (1988) Adriamycin-induced free radical formation in the perfused rat heart: Implications for cardiotoxicity, *Cancer Res.*, 48: 4766-4769.
- Ranguelova K, Suarez J, Magliozzo RS, and Mason RP (2008) Spin trapping investigation of the peroxide- and isoniazid radicals in Mycobacterium tuberculosis catalase-peroxide. *Biochemistry* 47: 11377-11385.
- Sikora AG, Gelbard A, Davies MA, Sano D, Ekmekcioglu S, Kwon J, Hailemichael Y, Jayaraman P, Myers JN, Grimm EA and Overwijk WW (2010) Targeted inhibition of inducible nitric oxide synthase inhibits growth of human melanoma in vivo and synergizes with chemotherapy. *Clinic Cancer Res* 16:1834-1844.
- Sinha BK (1995) Topoisomerase Inhibitors: Therapeutic Potentials. *Drugs* 49: 11-19.
- Sinha BK, Politi PM, Eliot HM, Kerrigan D, and Pommier, Y (1990) Structure-activity relationship, cytotoxicity and topoisomerase II dependent cleavage induced by pendulum ring analogs of etoposide. *Eur J Cancer* 26:590-593.
- Sinha BK (1980) Binding specificity of chemically and enzymatically activated anthracyclines anticancer agents to nucleic acids. *Chem Biol Interact* 30: 67-77.
- Sinha BK, Trush MA, Kennedy KA, and Mimnaugh EG (1984) Enzymatic activation and binding of adriamycin to nuclear DNA. *Cancer Res* 44:2892-2896.

- Sinha BK, Katki, AG, Batist G, Cowan KH, and Myers CE (1987) Differential formation of hydroxyl radicals by adriamycin in sensitive and resistant MCF-7 human breast tumor cells: Implication for the mechanism of action. *Biochemistry*, 26: 3776- 3781.
- Sinha BK, Haim N, Durse L, Kerrigan, D and Pommier, Y (1988) DNA strand breaks produced by etoposide (VP16-213) in sensitive and resistant human breast tumor cells: implications for the mechanism of action. *Cancer Res* 48:5096-6000.
- Sinha BK, Bhattacharjee S., Chatterjee S, Jiang JJ, Motten AG, Kumar A, Espey MG, and Mason RP (2013) Role of nitric oxide in the chemistry and anticancer activity of etoposide (VP-16,213). *Chem Res Toxicol* 26: 379-387.
- Tang CH, and Grimm EA (2004) Depletion of endogenous nitric oxide enhances cisplatin-induced apoptosis in a p53-dependent manner in melanoma cell lines. *J Biol Chem* 279: 288-298.
- Wink DA, Cook JA, Christodoulou D, Krishna, MC, Pacelli R, Kim S, Degraff W, Gamsom J, Vodovotz Y, Russo A, and Mitchell JB (1997) Nitric oxide and some NO donor compounds enhance the cytotoxicity of cisplatin. *Nitric oxide-Biology and Chemistry* 1:88-94.
- Wink DA, Vodovotz Y, Cook JA, Krishna MC, Kim S, Coffin D, DeGraff W, Deluca AM, Liebmann J, and Mitchell JB (1998) Role of nitric oxide chemistry in cancer treatment. *Biochemistry (Moscow)* 63:802-809.
- VanMaanen JMS, deVaries J, Pappie D, VandenAkker E, Lafeur MVM, Retel J, Vandergeef J and Pinedo HM (1987) Cytochrome OP450-mediated O-demethylation-a route in the metabolic activation of etoposide (VP-16231). *Cancer Res* 47: 4658-4662.

- Vlasova II, Feng, W-H, Goff, JP, Goff JP, Giorgianni A, Do D, Gollin SM, Lewis, DW, Kagan, VE and Yalowich JC (2011) Myeloperoxidase-dependent oxidation of etoposide in human myeloid progenitor CD34<sup>+</sup> cells. *Molecular Pharmacol* 79: 479-487.
- Xu WM, Liu LZ, Loizidou M, Ahmed M, and Charles IG (2002) The role of nitric oxide in cancer. *Cell Research* 12: 311-320.
- Yang DT, Yin JH, Mishra S, Mishra R, and Hsu CY (2002) NO-mediated chemoresistance in C6 glioma cells. *Ann NY Acad Sci* 962: 8-17.
- Yenes S, and Messeguer A (1999) A study of the reaction of different phenol substrate with nitric oxide and peroxynitrite. *Tetrahedron* 55:14111-14122.
- Zhuang L, Lin JQ, Lu ML, Solomon KR, and Freeman MR (2002) Cholesterol-rich lipid rafts mediate akt-regulated survival in prostate cancer cells. *Cancer Res.* 62: 2227-2231.

**Funding Support:** This research was supported [in part] by the intramural research program of the NIH, National Institute of Environmental Health Sciences.

## Figure Legends:

**Figure 1, Panel A:** The Western blots for iNOS and effects of LPS (10 ng/ml) in A375 cells.

**Panel B:** Quantitation of the iNOS protein in A375 cells using rabbit polyclonal anti-iNOS antibody in the standard ELISA assay as described in the Methods section. For the Western blots, A375 cells were seeded at  $1 \times 10^6$  in a six-well plate. LPS (10 ng/ml) was added and exposed for 14-16 h. Cells were collected, lysed and examined for iNOS protein by Western blots. For the Western blots, 10  $\mu$ g of proteins were loaded, and actin was used to assess equal loading of the proteins. Data are means of 3 separate experiments carried out in duplicate. The significance (\*\*  $p < 0.005$ ) compared to the untreated control.

**Figure 2, Panel A:** The caspase-3 assay as an indicator of VP-16 apoptosis in the presence or absence of iNOS inhibitors was carried out according to the manufacturer's protocol. L-NIL (400  $\mu$ M) was dissolved in the medium and added to A375 cells ( $1 \times 10^6$ /well) in 6-well plates and incubated for 4 h before adding VP-16. The cells were incubated for another 18 h before collecting cells by centrifugation. Data are the means of 3 separate experiments carried out in duplicate. Significance (\*  $p < 0.05$ ,  $n = 3$ ) was determined by Student's t-test. **Panel B:**

Cytotoxicity studies with VP-16 in human A375 cells in the presence or absence of L-NIL (400  $\mu$ M) were carried out using the MTT assays described in the Methods section.

Cytotoxicity data are the means of 4 separate experiments carried out in triplicate.

Significance (\*  $p < 0.05$ ,  $n = 4$ ) against concentration-matched VP-16 alone was determined by Student's t-test.

**Figure 3, Panel A:** Cytotoxicity of VP-16 in A375 cells following induction with LPS (10 ng/ml 16 hrs.) and effects of L-NIL (400  $\mu$ M) on VP-16 cytotoxicity using the MTT assay as

described in Figure 2. Data are means of 3 separate experiments carried out in triplicate. Significance (\*  $p < 0.05$ ,  $n = 3$ ) against concentration-matched VP-16 alone and VP-16 + L-NIL was determined by Student's-t-test. **Panel B:** Cytotoxicity of VP-16 in A375 cells in the presence of LPS-induced RAW cells ( $1 \times 10^6$  cells/incubation). Co-culture studies were conducted as described in the Methods section. Data are means of 3 separate experiments carried out in duplicate. Significance (\*  $p < 0.05$  and \*\*  $p < 0.005$ ,  $n = 3$ ) against concentration-matched VP-16 alone was determined by Student's t-test.

**Figure 4:** Caspase-3 activity as an indicator of apoptosis (A) and cytotoxicity (B) induced by Adriamycin, respectively, in A375 cells. These studies were carried out as described in Figure 2. Data are means of 3 separate experiments carried out in triplicate for the cytotoxicity and in duplicate for the caspase-3 activity. Significance (\*\*  $p < 0.005$ ,  $n = 3$  compared to control) was determined by Student's t-test.

**Figure 5, Panel A:** Measurement of the VP-16 cleavable complex formation. The SDS-KCl precipitation assay with VP-16 in the presence of L-NIL was carried out as described in the methods section. L-NIL (400  $\mu\text{M}$ ) was incubated with the cells for 18 h during the labeling phase before VP-16 was added for 1 h. \*  $p < 0.05$ ,  $n = 3$  compared to controls and 10  $\mu\text{M}$  VP-16 treatment and 50  $\mu\text{M}$  + L-NIL treatment compared to 50  $\mu\text{M}$  VP-16 treatment alone. **Panel B:** Co-culture experiments for determination of SDS-KCl precipitate formation were carried out with LPS-induced (1  $\mu\text{g}/\text{ml}$  for 14-16 h) RAW cells as described in the Methods section. Significance (\*\*  $p < 0.005$ ,  $n = 3$  compared to control and VP-16 treated simultaneously or preincubated; \*  $p < 0.05$ ,  $n = 3$  compared to control) was determined by Student's t-test.

**Figure 6:** HPLC analysis of the cellular metabolism of VP-16 (100  $\mu$ M) in the presence or absence of L-NIL (400  $\mu$ M). A375 cells were incubated with L-NIL for 18 h before VP-16 was added and incubated for 15 minutes afterwards. Metabolites were isolated as described in the Methods section and analyzed by HPLC. The solid line represents cells treated with VP-16 only, and the dashed line represents cells treated with both VP-16 and L-NIL. Insert: The HPLC analysis of products formed *in vitro* during reactions of  $\bullet$ NO gas with VP-16 at a low ratio in chloroform as described before (Sinha et al., 2013).

**Table-1:** Cytotoxicity of VP-16 in human A375 melanoma cells under various treatment conditions.

Conditions	IC <sub>50</sub>
VP-16	$2.5 \pm 0.5 \times 10^{-7}$ M
VP-16 + L-NIL	$8.5 \pm 0.5^* \times 10^{-8}$
VP-16	$2.5 \pm 0.5 \times 10^{-7}$ M
VP-16 + LPS	$9.0 \pm 0.8^* \times 10^{-7}$ M
VP-16 + LPS + L-NIL	$2.0 \pm 0.5^* \times 10^{-7}$ M
VP-16	$5.2 \pm 0.5 \times 10^{-7}$ M
VP-16 + Induced RAW Cells	$8.5 \pm 0.70^{**} \times 10^{-6}$ M

Cytotoxicity studies were carried out as described in the Methods section and also detailed in their respective figures. Data are means of 3-4 separate experiments. Significance (\*p < 0.05 and \*\*p < .005) was determined by Student's t-test.

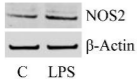
Table-2: Relative nitrite concentration during co-culture studies for cytotoxicity with VP-16 in A375 cells in the presence of LPS-induced RAW Cells.

Conditions	Top	Bottom
Control, Untreated	52.43 $\pm$ 1.0	52.32 $\pm$ 0.8
+ 50 $\mu$ M VP-16	25.35 $\pm$ 2.1 <sup>**</sup>	24.7 $\pm$ 2.4 <sup>**</sup>
+ 10 $\mu$ M VP-16	31.7 $\pm$ 1.6 <sup>**</sup>	25.3 $\pm$ 1.0 <sup>**</sup>
+ 1 $\mu$ M VP-16	37.5 $\pm$ 1.0 <sup>**</sup>	31.8 $\pm$ 1.0 <sup>**</sup>
+ 0.1 $\mu$ M VP-16	36.5 $\pm$ 1.0 <sup>*</sup>	36.7 $\pm$ 1.0 <sup>*</sup>

Nitrite concentrations were determined using Greiss Reagent by removing samples (100  $\mu$ l; 4 h) from the top and bottom layers (separated by 0.4  $\mu$ M membrane filters, Costar, Corning, NY) in six-well plates. A375 cells were seeded in the bottom layer and the LPS-induced RAW cells were seeded on the top. The concentration of nitrite is expressed as  $\mu$ M/10<sup>6</sup> RAW cells. Data are means of 3 separate experiments. Significance (\*p < 0.05 and \*\*p < .005; compared to untreated controls) was determined by Student's t-test.

Figure 1

**A**



**B**

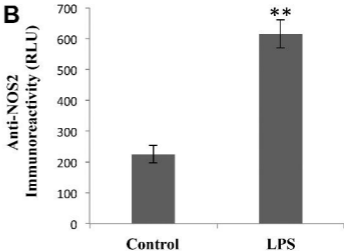
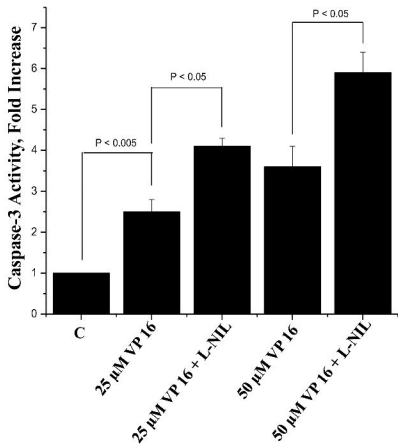


Figure 2

**A**



**B**

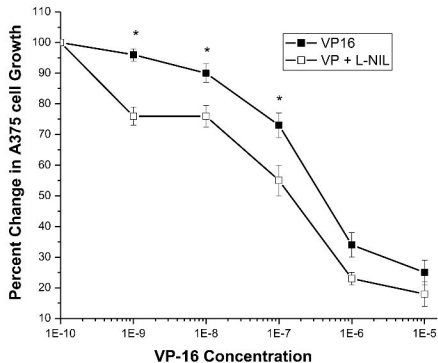
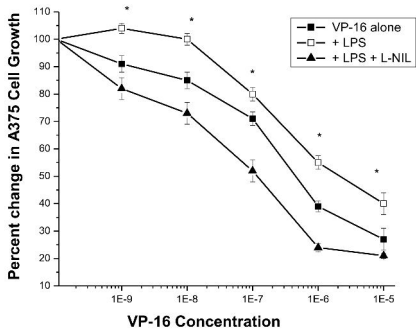


Figure 3

**A**



**B**

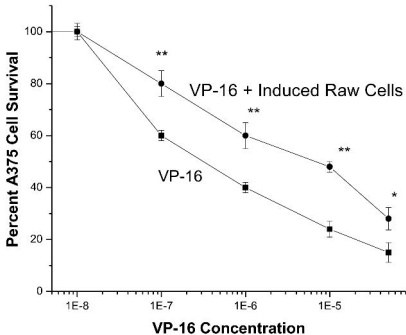
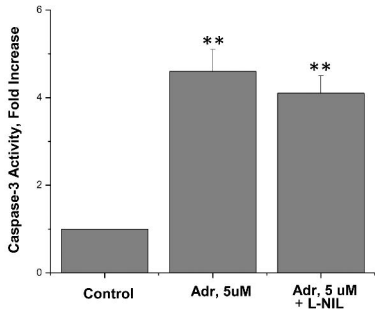


Figure 4

**A**



**B**

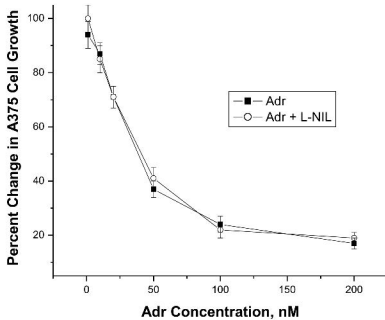
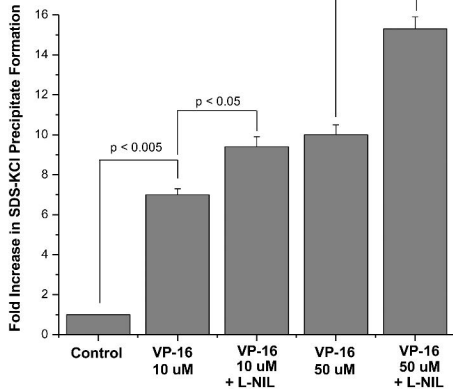


Figure 5

**A**



**B**

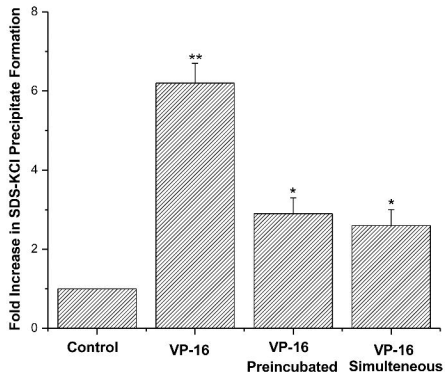


Figure 6

